第 31 卷第 4 期
2015 年 4 月

无 机 化 学 学 报
CHINESE JOURNAL OF INORGANIC CHEMISTRY

Vol.31 No.4
641-648

硫/水热碳球复合材料的制备及对锂硫电池倍率性能的影响

李严冰 段晓波 韩亚苗 朱 丁 黄利武 陈云贵*
(四川大学材料科学与工程学院,成都 610065)

摘要:在锂硫电池正极材料的研究中,碳材料可以有效改善电池倍率及循环性能。为了提高锂硫电池的高倍率放电性能,通过水热合成的方法,制备了由非均匀粒径碳球组成的碳材料。与硫热合成后,硫均匀分布在碳材料表面及周围,复合材料含硫量为52wt%。0.2C 放电电流下,首次放电比容量为 1 174 mAh·g^{-1},100 次循环后放电比容量为 788 mAh·g^{-1}。在 4C 的放电电流下,放电比容量稳定维持在 600 mAh·g^{-1},循环过程中,库伦效率高于 90%。该碳材料有良好的导电网络,且制备方便,成本低廉,对于穿梭效应和放电过程中的膨胀效应有一定的抑制作用,是一种优秀的正极材料。

关键词:锂硫电池;水热法;硫碳复合材料;高倍率
中图分类号:O614.111;O613.51;O613.71 **文献标识码**:A **文章编号**:1001-4861(2015)04-0641-08
DOI:10.11862/CJIC.2015.073

Sulfur-Hydrothermal Carbon Composites for Cathode in High-Rate Lithium-Sulfur Batteries

LI Yan-Bing DUAN Xiao-Bo HAN Ya-Miao ZHU Ding HUANG Li-Wu CHEN Yun-Gui*
(*College of Materials Science and Engineering, Sichuan University, Chengdu* 610065, *China*)

Abstract: Sulfur-carbon composites as the cathode of Lithium-Sulfur batteries have shown excellent electrochemical performance for high power devices. To enhance rate performance of sulfur cathode for Li-S batteries, a carbon material consisted of non-uniform carbon spheres has been prepared by hydrothermal method. Sulfur disperses evenly on the surface of the carbon spheres via a melt-diffusion method. The as-prepared composite with a sulfur content of 52wt% delivers an initial discharge capacity of 1 174 mAh·g^{-1} and a reversible discharge capacity of 788 mAh·g^{-1} after 100 cycles at 0.2C. At a higher rate of 4C, the capacity stabilizes at around 600 mAh·g^{-1}. During cycling, the coulombic efficiency is maintained above 90%. The results show that the carbon-sulfur composites with chain conductive network represents a promising cathode material for rechargeable lithium batteries because of the effective improvement of the electronic conductivity, the restraint of the volume expansion and the reduction of the shuttle effect.

Key words: lithium-sulfur batteries; hydrothermal; sulfur/carbon composite; high-rate

0 Introduction

As hybrid electric vehicles (HEVs) and portable electronic devices are making their entry into the market and our lives, the demand for high energy rechargeable batteries continues to rise[1-3]. The current lithium-ion batteries(LIBs) can offer a practical specific energy only around 150 Wh·kg^{-1}. Therefore, rechargeable batteries beyond LIBs have been investigated as alternatives. Among them, lithium-sulfur (Li-

收稿日期:2014-09-25。收修改稿日期:2015-01-01。
*通讯联系人。E-mail:ygchen60@aliyun.com,Tel:0086-28-85407335

S) battery has received considerable attention[4-5].

Rechargeable Li-S batteries are safe, environmentally friendly and low cost. The high specific capacity (1 675 $mAh \cdot g^{-1}$) coupled with a cell voltage of about 2.15 V leads to theoretical energy density of 2600 $Wh \cdot kg^{-1}$, which is almost seven times higher than that of the current LIBs ($\approx$387 $Wh \cdot kg^{-1}$)[6-9]. However, there are still challenges in obtaining good cycling stability at high power. Good cycling stability is essential for real applications such as automotive transport. Compared with other cathode materials such as $LiCoO_2$, both sulfur and lithium polysulfide are electronic insulators, and sulfur is not ionically conductive either[10-14]. Another issue is the "shuttle effect". Lithium polysulfides (Li_2S_n, $2<n\leqslant 8$) are soluble in most electrolytes. It causes a decrease of active material, capacity fading, inactivation of the anode, and self-discharge of the cell[15-19].

Approaches for improving the performance of the sulfur cathode are to replace the carbonate-based solvents with ionic or polymeric liquid solvents[19-20] so that the diffusivity and solubility of the polysulfides would be slowed down thus setting up a physical[21-23] or chemical[24] obstacle in cathode for adsorbing the polysulfide. The previous strategy is to increase electrical resistivity and the viscosity of electrolytes. Thus, it is not appropriate for fast discharge and charge. Metal oxides or polymers face the same problem. For example, their insulating nature makes the reaction very slow except for small amounts. Carbonaceous materials with good electrical conductivity, large surface area, strong adsorption properties, and short transport pathways for both electrons and Li ions are more favorable choices to deal with the challenges. Lots of carbon-sulfur composites use impregnation via filling carbon pores with molten sulfur[25]. Nevertheless, the fully filled pores block the penetration of lithium ions and electrolyte thus increasing cathode polarization. It could limit the power performance of sulfur cathodes. Furthermore, to satisfy the commercial requirements in the future, the compacted density of carbon materials should be more promising compared with some porous carbon or carbon black with a low density. Thus, carbon material with a spherical morphology as an electrically conductive matrix is considered to be an option of the sulfur cathode.

Here, we report a composite of sulfur evenly dispersed on the surface of the carbon material as the cathode for Li-S batteries. The carbon material was prepared through hydrothermal method and showed a degree of graphitization. The carbon-sulfur composite was synthesized by heat treatment. The composite with 52wt% sulfur shows a good electrochemical properties.

1 Experimental

1.1 Preparation of carbon spheres

6.2 g of glucose was put in 50 mL of deionized water. Then the obtained solution was placed into a sealed autoclave and heated at 200 ℃ with a pressure of 2 MPa in the hydrothermal synthesis reactor for 4~8 h. After cooling down to room temperature, the caramel color products were collected by an air pump filter and then washed with deionized water. After repeated washing, the product was dried in a vacuum oven at 60 ℃ for 24 h, and then heated at 750 ℃ for 5 h in a tube furnace under the atmosphere of Argon.

1.2 Preparation of sulfur/carbon composites

The prepared carbon materials (0.5 g) were mixed with sublimed sulfur (1 g). In order to confirm the improvement of the electrochemical performance by the material itself rather than the carbon content, the reference sample was the sublimed sulfur mixed with the commonly used carbon material Super P in the same weight ratio of 2∶1 (the S/Super P composite). The two S/C mixtures were heated at 155 ℃ for 12 h in sealed container filled with argon. At this temperature, the sulfur has the lowest viscosity. Then, the temperature was raised to 300 ℃ and kept for 1 h. the sulfur-carbon spheres (S/CS) composite and the S/Super P composite were obtained after cooling the system to room temperature.

1.3 Assembly of Li-S cells

The two composites were mixed with Super P and polyvinylidene fluoride (PVDF 2801) in a weight ratio

of 80:10:10, with *N*-methyl-2-pyrrolidone (NMP) as a dispersant. The cathode electrodes were made by coating the slurry on aluminum foil (20 μm) with KTQ-Ⅱ adjustable coating machine and dried at 60 ℃ for 20 h in the oven (DZF-6020). CR2025 coin-type cells were assembled to test the electrochemical performance of the sulfur-carbon cathode materials with lithium metal (14 mm in diameter) as the anode, and a Celgard 2400 as the separator. The electrolyte was 0.65 mol·L^{-1} lithium bis (trifluoromethanesulfonyl) imide (LiTFSI) in a mixed solvent of 1,2-dimethoxyethane (DME) and 1,3-dioxolane (DOL) (*V*/*V*, 1:1, Beijing Chemical Reagent Research Institute). After assembly, a 3 h standing for the cells was allowed to ensure the immersion of electrolyte into the electrodes.

1.4 Characterizations

X-ray power diffraction (XRD-DX-2600) was performed with graphite monochromator and Cu *Kα* radiation (λ=0.154 18 nm) at a scan rate of 0.04°·s^{-1} at operating voltage of 35 kV and the current of 25 mA. Scanning electron microscopy was SEM-JSM-6490LV, and thermogravimetry (NETZSCH STA 449F3) was operated under Ar at a scan rate of 10 ℃·min^{-1}. Raman spectroscopy (LabRAM HR) was performed with 532 nm diode laser excitation on a 300 lines mm^{-1} grating at room temperature. The relative properties of the hydrothermal carbon were characterized with MODEL FZ-2010 Semiconductor Power Resistivity Meter.

The coin cells were tested in galvanostatic mode at various currents at room temperature within a voltage window of 1.0~3.0 V using LAND 2001A battery tester. Cyclic voltammetry (CV) measurements were carried out with the coin cell at a scan rate of 0.5 mV·s^{-1} by using a Parstate 2273 electrochemical workstation.

2 Results and discussion

2.1 Structure characterization

Fig.1a exhibits the XRD patterns of the as-prepared carbon spheres, sublimed sulfur and S/CS composite. The XRD pattern of elemental sulfur shows two sharp diffraction peaks at 2*θ*=23° and 28°, indicating an orthorhombic structure. The XRD pattern of the as-prepared carbon shows two broad peaks around 23° and 44°, which correspond to the (002) and (100) diffraction, respectively. The (100) diffraction indicates an amorphous framework, while (002) diffraction suggests a certain degree of graphitized structure with high electronic conductivity. As for the S/CS composite, the diffraction peaks of the sulfur are still present, but the intensities become lower. Fig.1b shows the results obtained from TG of the prepared S/CS composite, S/Super P composite, and sublimed sulfur correlated to the sublimation of sulfur under argon atmosphere. The sulfur content is about 52wt% and 50wt%, respectively for the S/CS composite and the S/Super P electrode.

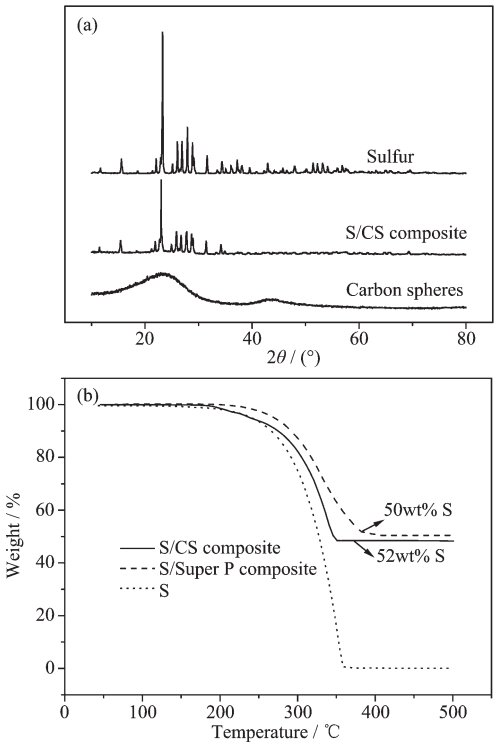

Fig.1 XRD patterns of sublimed sulfur, the carbon spheres and the S/CS composite (a); TG curves of the S/CS composite and the S/Super P composite and sulfur taken under Ar at a rate of 10 ℃·min^{-1} (b)

Raman spectrum for the hydrothermal carbon is shown in Fig.2. The spectrum is obtained with 532 nm diode laser excitation on a 300 lines mm^{-1} grating at room temperature. The Raman spectrum of the hydrothermal carbon shows typical pattern of partially graphitized carbon. Two main bands are seen in the spectrum, the D band and the G band. The G band at

around 1 600 cm^{-1} is due to a bond stretching vibration of a pair of sp^2 sites corresponding to graphitic cluster lattice vibration mode with E_{2g} symmetry. The D band at 1 350 cm^{-1} is due to an A_{1g} breathing vibration of a six-fold aromatic ring that is activated by disordered carbon. I_D and I_G in the Raman spectrum provide the degree of graphitization and the size of any graphitic clusters in disorder carbon. The I_D is stronger than I_G, suggesting that the hydrothermal carbon has a structure with a fraction of graphitic cluster dispersed in disordered carbon.

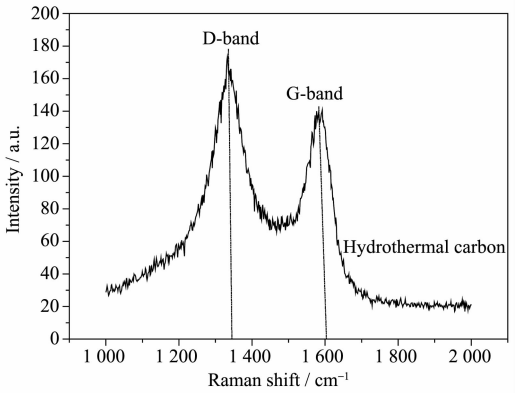

Fig.2 Raman spectrum of the hydrothermal carbon

As shown in Fig.3a, the Super P consists of carbon particles of different sizes, and the particles are independent of each other. After mixing with sulfur and the heat treatment, as seen in Fig.3b, sulfur evenly distributes on the surface of carbon particles. The C and S elements mapping shown in Fig.3c and Fig.3d also proves it. The Fig.3e is a sketch map of the Super P/S composite, it shows the distribution of the S and C in the composite clearly. When sulfur is attached to the surface of carbon particles, the contact between carbon particles will be weakened, severely reducing the conductivity of the conductive network.

Fig.4a and 4b show that the carbon material has a sphere-like morphology with a size from submicron to micron order. The formation of non-uniform carbon spheres is due to the use of excessive glucose in the preparing process, so that large particles of carbon spheres will be generated because of the high temperature with long holding time. Carbon spheres of various particle sizes do not exist independently.

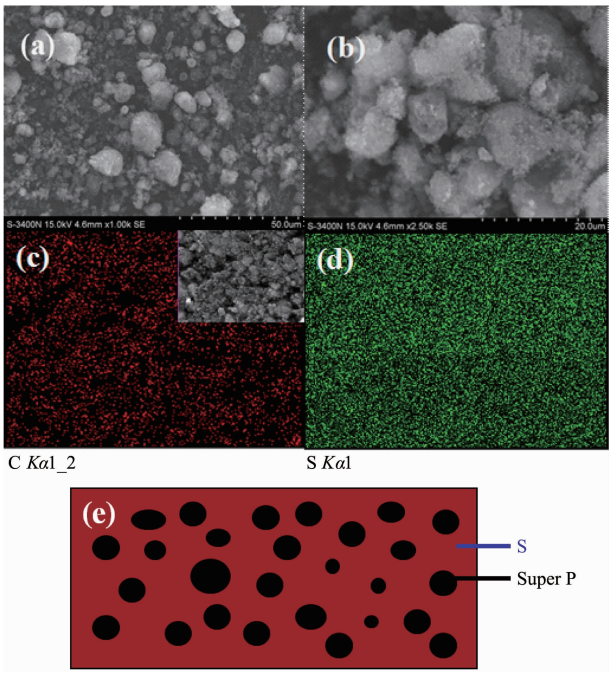

Fig.3 SEM images of Super P (a), S/Super P composite (b), elemental maps of Super P (c) and S (d) in the Super P/S composite, Sketch map of the Super P and S distribution in the composite (e)

Among these carbon spheres, there is a chain conductive network, as shown in Fig.4g, which improves both electron conduction and ionic conduction. The hydrothermal product is obtained by filtering, rather than by high speed centrifugation thus leading to the formation of the network. The specific resistivity of the hydrothermal carbon is 0.026 Ω·cm, and the Super P is 0.053 Ω·cm. The voids between the carbon spheres provide more reaction sites for the electrochemical reaction. After the heat treatment for sulfur and carbon spheres, as seen in Fig.4c, there still exists some space, which slows down the pore blockage caused by the deposition of the resultant on the surface at high rate discharge and by effective buffer volume expansion during the reaction, thus ensuring the stability of the structure. By contrast, the contact between Super P particles depends mainly on the PVDF binder, but the binder is not stable in the reaction process, which leads to instability of the cathode structure. Fig.4e and 4f are the elemental maps of the carbon and sulfur for the S/CS composite. Obviously, the elemental map confirms that the sulfur

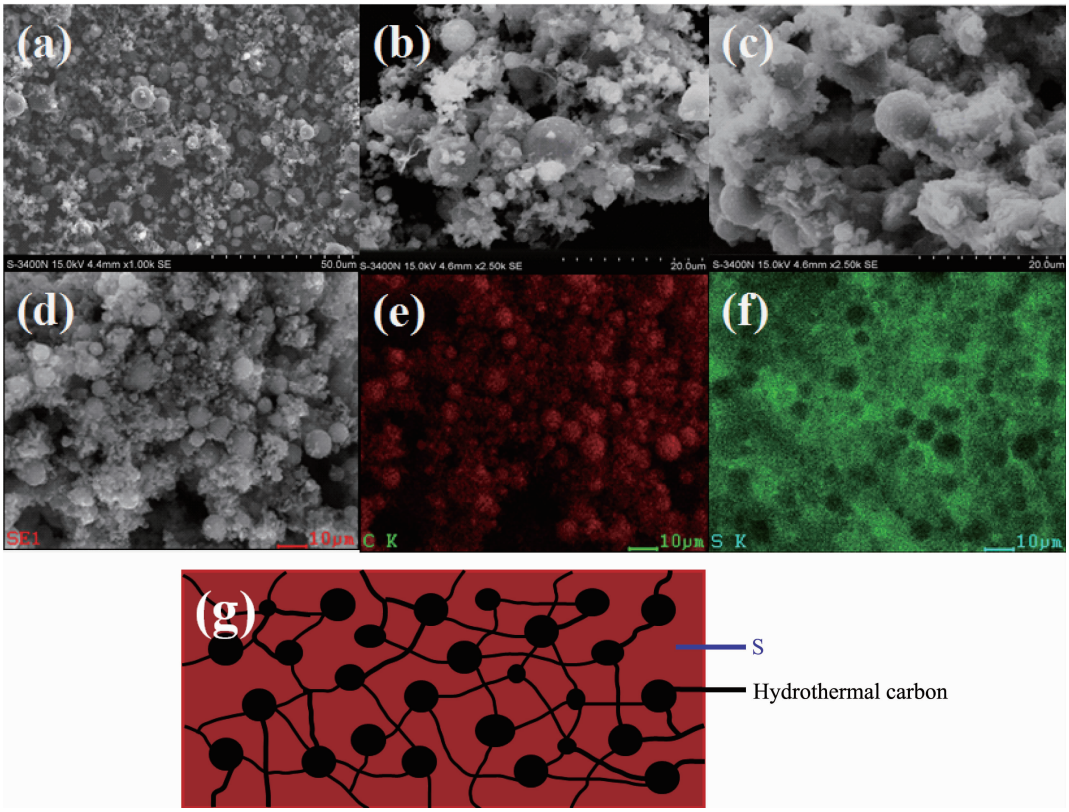

Fig.4　SEM images of carbon spheres (a); Carbon spheres under different magnifications (b); SEM images of S/CS composite (c); Elemental maps of carbon (e) and sulfur (f) in the S/CS composite corresponding to (d); Sketch map of the Super P and S distribution in the composite (g)

is homogeneously distributed in the framework of the carbon sphere material.

2.2　Electrochemical performance

In Fig.5a, the S/CS composite shows a good high-rate performance. At the maximum discharge rate of 4C, it delivers a reversible capacity (calculated on the basis of sulfur) of 683 $mAh \cdot g^{-1}$ (1 675 $mAh \cdot g^{-1}$ at 1C). With the increase of the discharge rate, the discharge capacity decreases accordingly. However, at the same discharge rate, the specific discharge capacity is relatively stable. The stability of the cathode material is also evidenced by the recovery of capacity when the rate goes back to 0.2C. This is because that the carbon material as a matrix can provide a good electrical conductivity and a stable structure. At the same time, the high dispersion of elemental sulfur in the carbon materials is good for the high-rate discharge capability of the sulfur cathode. Fig.5b shows the discharge-charge plots at a serious of current density. As can be seen, with the increase of current density, discharge plateaus are gradually reduced, when the current goes to 4C, voltage plateau is about 1.7 V. As a comparison, the S/Super P electrode delivers a reversible capacity even more than that of the S/CS composite under the discharge rate of 0.2C. As shown in Fig.5c, when the discharge current gets higher, the capacity of the S/Super P electrode declines seriously, the corresponding voltage plateau reduces obviously, too. When the discharge current increases to 2C, the voltage plateau is almost disappeared. The polarization during high-rate cycling is also much more serious than that of the S/CS composite electrode.

As seen in Fig.6a, the S/CS composite delivers a discharge capacity of 1 174 $mAh \cdot g^{-1}$ at 0.2C in the 1st cycle. After that, it shows a good electrochemical reversibility with a capacity of about 1 041 $mAh \cdot g^{-1}$ in the 2nd cycle, 788 $mAh \cdot g^{-1}$ in the 100th cycle, and the capacity retention is 67%, which means that it has a good utilization of sulfur. The corresponding

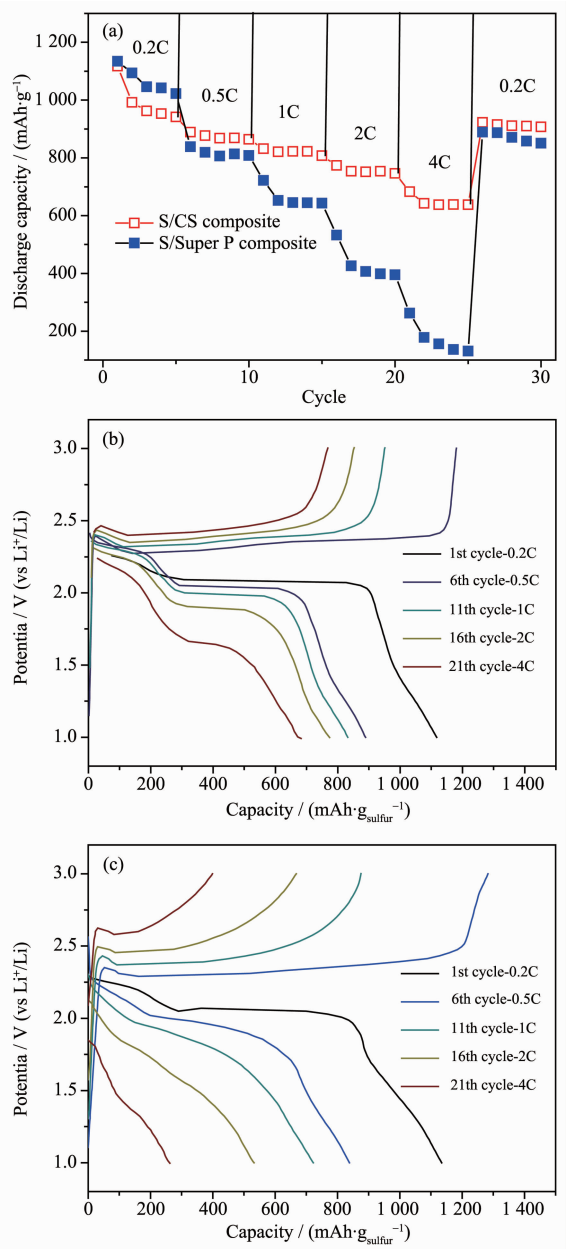

Fig.5 Rate performance of the S/CS composite and the S/Super P electrode at different C rates (a); voltage vs capacity profiles of the S/CS composite (b) and the S/Super P electrode (c) at different discharge rates

coulombic efficiency is maintained above 90% during cycling, indicating that this material has played a good role in limiting the dissolution and diffusion of polysulfide lithium. It reduces the shuttle effect effectively. Because the percentage of sulfur and carbon in the two S/C composites are similar, the S/Super P electrode delivers a capacity nearly as much as the S/CS composite in the first few cycles, but as the reaction proceeds, its capacity suffers heavy losses. After 100 cycles, the capacity retention is only 26%, and the coulombic efficiency is far below that of the S/CS electrode. Fig.6b shows the cycle performance of the S/CS electrode at a higher current density of 2C. After 200 cycles, it still delivers a specific capacity of 518 mAh·g^{-1}, the capacity retention is 73%. The coulombic efficiency is maintained above 95% during 200 cycles. This is because that as the current density increases, the electric field force also increases, which inhibits the shuttle effect to a certain extent. The typical discharge-charge curves of the S/CS composite with 52wt% sulfur at 0.2C are shown in Fig.6c. Two discharge voltage plateaus appear at about 2.3 V and 2.0 V. The higher plateau indicates the S_8 ring opening to the linear high order lithium polysulfides (Li_2S_x, $4<x<8$), the lower one is about the further reduction of Li_2S_x ($4<x<8$) to Li_2S_2 and Li_2S, which is assigned to a two-step reaction of a discharge process.

Fig.6d shows the CV curves of the S/CS composite electrode during the first 3 cycles. The peaks of the curve correspond very well with voltage plateaus in the discharge-charge plots in Fig.6c. Two cathodic peaks at ~2.3 V and ~2.0 V in CV plots are observed due to the multiple reduction of sulfur with Li^+ ions. In the procedure of anodic scanning, only one peak at ~2.5 V is observed, which stands for the oxidation of Li_2S_2 and Li_2S to Li_2S_8. Maybe it is because that the high potential polarization between the insoluble lithium sulfide and lithium polysulfides makes the two oxidation peaks overlapped. In Fig.6c, the two plateaus have a close interval of potential in keeping with that only one anodic peak is observed on the oxidization side of the CV curve. Over 3 cycles, both the CV peak positions and the peak currents change slightly, demonstrating that the cathode materials have excellent electrochemical reversibility which can be attributed to its structure and good electronic conductivity of the S/CS composite.

Obviously the mass loss and the solubility of active materials could have a significant impact on the sulfur cathode, but the rate and cycle performance is

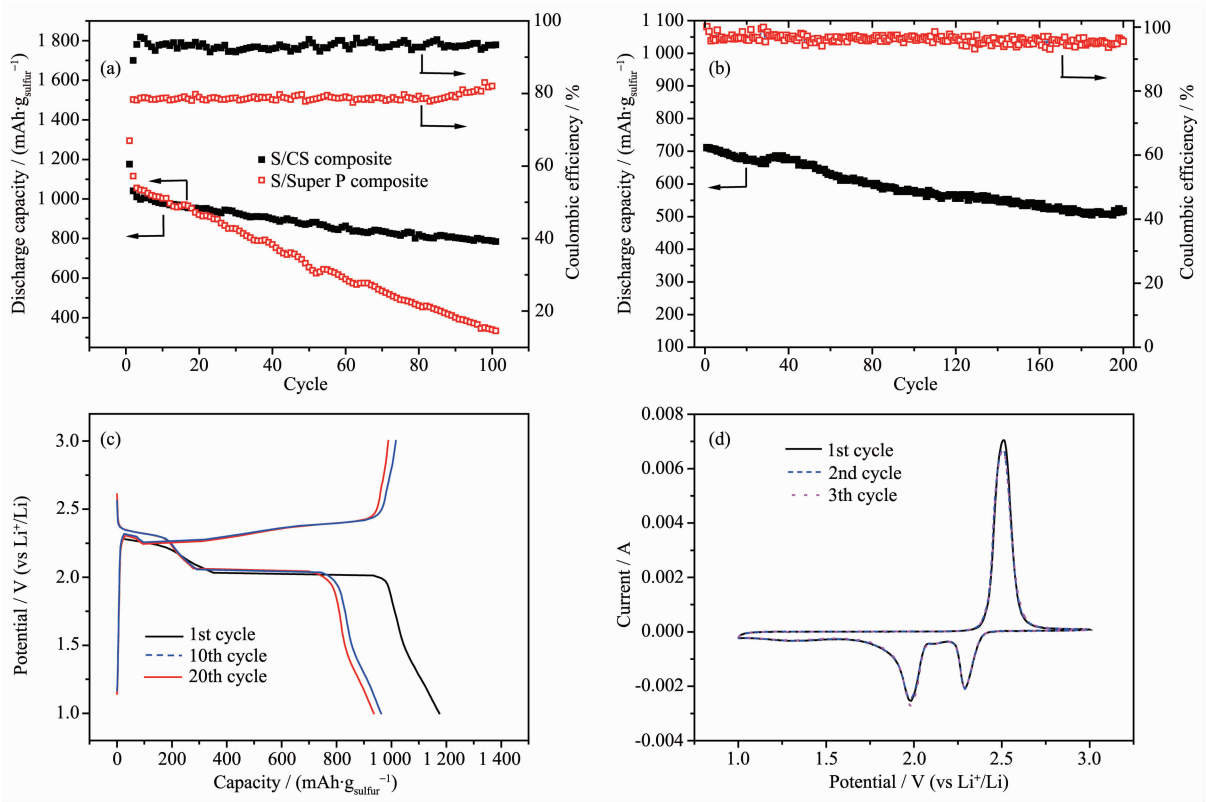

Fig.6　Cycle performance and its corresponding coulombic efficiency of the S/CS and the S/Super P composite electrode at 0.2C (a) and the S/CS composites at 2C (b); voltage vs capacity curves of the S/CS composite at 1st, 10th, 20th cycle at 0.2C (c); CV profiles of the S/CS composite electrode when measured at a scan rate of 0.5 mV·s^{-1} in the potential range of 1.0~3.0 V (vs Li/Li$^+$) (d)

also related with the interface reaction. In order to verify that the prepared S/CS material is responsible for the performance of the cell with the electrode, we conducted electrochemical impedance spectroscopy (EIS). Fig.7 shows that all the Nyquist plots of sulfur cathodes are composed of a semicircle in the high frequency region and a linear in the low frequency region. The semicircle is about the interface charge-transfer process of the S/CS cathode. The greater of the semicircle diameter indicates the greater resistance of the electrodes of the electrochemical reaction. The straight line corresponds to the ion diffusion resistance, which is called Warburg diffusion. It is obvious that the S/CS composite electrode exhibits a much smaller charge transfer resistance than that of the S/Super P electrode, although its carbon content is lower. The diameter of the semicircle before cycling is significantly larger than that of the semicircle after the 1st cycle, because the active material of initial state is sulfur, but the active material after the 1st cycle is lithium polysulfide. Obviously, the enhanced structural stability and electrical conductivity of the carbon material as matrix makes a contribution to improve the electrochemical performance of the sulfur cathode. Furthermore, this can be well matched with the

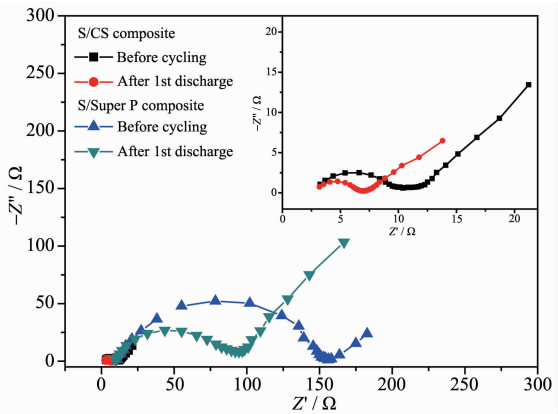

Fig.7　EIS spectra of the S/CS and S/Super P composite electrode at the current density of 0.5C; Inset: the detail for high frequency area

electrochemical performance.

3 Conclusions

The carbon-sulfur composites were synthesized by a melt-diffusion of sulfur in hydrothermal carbon, and the weight ratio of sulfur is 52% in the composite. The obtained structure of carbon-sulfur composites is effective in improving the electrochemical performance of S-based cathode material. The electronic/ionic transport and the ability to accommodate volume expansion in the reaction process are also improved owing to the unique chain conductive network structure of the carbon matrix. The sulfur cathode exhibits specific capacity retention of ~66% at 0.2C after 100 cycles, ~73% at 2C after 200 cycles, and the coulombic efficiency maintains above 90% in the cycles. At the discharge current of 4C, it still delivers a specific capacity of more than 600 $mAh \cdot g^{-1}$. As a result, when evaluated as a cathode material for lithium-sulfur batteries, the S/CS composite shows good electrochemical performance with excellent rate capability and cycling stability.

References:

[1] Manthiram A, Fu Y, Su Y S. *Acc. Chem. Res.*, **2012**,**46**:1125-1134

[2] Bruce P G, Freunberger S A, Tarascon J M, et al. *Nat. Mater.*, **2012**,**11**:19-29

[3] Lu Y C, He Q, Gasteiger H A. *J. Phys. Chem. C*, **2014**,**118**:5733-5741

[4] Cheon S E, Choi S S, Han J S, et al. *J. Electorchem. Soc.*, **2004**,**151**(12):A2067-A2073

[5] Evers S, Nazar L F. *Acc. Chem. Res.*, **2012**,**46**(5):1135-1143

[6] He G, Ji X, Nazar L. *Energy Environ. Sci.*, **2011**,**4**:2878-2883

[7] Choi Y J, Chung Y D, Baek C Y, et al. *J. Power Sources*, **2008**,**184**(2):548-552

[8] Liang X, Wen Z, Liu Y, et al. *J. Power Sources*, **2011**,**196**:3655-3658

[9] Geng X, Rao M, Li X, et al. *J. Solid State Electrochem.*, **2013**,**17**:987-992

[10]Lu S, Cheng Y, Wu X, et al. *Nano Lett.*, **2013**,**13**(6):2485-2489

[11]Rauh R D, Abraham K M, Pearson G F, et al. *J. Electrochem. Soc.*, **1979**,**126**(4):523-527

[12]He X, Pu W, Ren J, et al. *Ionics*, **2008**,**14**(4):335-337

[13]Zhu Y, Zhang L, Schappacher F M, et al. *J. Phys. Chem. C*, **2008**,**112**(23):8623-8628

[14]Zhang B, Qin X, Li G R, et al. *Energy Environ. Sci.*, **2010**,**3**(10):1531-1537

[15]Jayaprakash N, Shen J, Moganty S S, et al. *Angew. Chem. Int. Ed.*, **2011**,**123**(26):6026-6030

[16]Shin J H, Jung S S, Kim K W, et al. *J. Mater. Sci.-Mater. El.*, **2002**,**13**(12):727-733

[17]Wei S, Zhang H, Huang Y, et al. *Energy Environ. Sci.*, **2011**,**4**(3):736-740

[18]Su Y S, Manthiram A. *Chem. Commun.*, **2012**,**48**(70):8817-8819

[19]Marmorstein D, Yu T H, Cairns E J, et al. *J. Power Sources*, **2000**,**89**(2):219-226

[20]Shin J H, Cairns E J. *J. Electrochem. Soc.*, **2008**,**155**(5):A368-A373

[21]Zheng G Y, Yang Y, Cha J J, et al. *Nano Lett.*, **2011**,**11**(10):4462-4467

[22]Ji X, Evers S, Black R, et al. *Nat. Commun.*, **2011**,**2**:325-331

[23]Ji X L, Lee K T, Nazar L F. *Nat. Mater.*, **2009**,**8**(6):500-506

[24]Demir-Cakan R, Morcrette M, Nouar F, et al. *J. Am. Chem. Soc.*, **2011**,**133**:16154-16160

[25]Liang C D, Dudney N J, Howe J Y. *Chem. Mater.*, **2009**,**21**(19):4724-4730